Atmos. Chem. Phys., 12, 9441–9458, 2012
www.atmos-chem-phys.net/12/9441/2012/
doi:10.5194/acp-12-9441-2012

Atmospheric Chemistry and Physics

The impact of differences in large-scale circulation output from climate models on the regional modeling of ozone and PM

A. M. M. Manders[1], E. van Meijgaard[2], A. C. Mues[3], R. Kranenburg[1], L. H. van Ulft[2], and M. Schaap[1]

[1]TNO, P.O. Box 80015, 3584 TA Utrecht, The Netherlands
[2]KNMI, De Bilt, The Netherlands
[3]FUB, Berlin, Germany

Correspondence to: A. M. M. Manders (astrid.manders@tno.nl)

Received: 2 March 2012 – Published in Atmos. Chem. Phys. Discuss.: 11 May 2012
Revised: 26 September 2012 – Accepted: 30 September 2012 – Published: 19 October 2012

Abstract. Climate change may have an impact on air quality (ozone, particulate matter) due to the strong dependency of air quality on meteorology. The effect is often studied using a global climate model (GCM) to produce meteorological fields that are subsequently used by chemical transport models. However, climate models themselves are subject to large uncertainties and fail to reproduce the present-day climate adequately. The present study illustrates the impact of these uncertainties on air quality. To this end, output from the SRES-A1B constraint transient runs with two GCMs, i.e. ECHAM5 and MIROC-hires, has been dynamically downscaled with the regional climate model RACMO2 and used to force a constant emission run with the chemistry transport model LOTOS-EUROS in a one-way coupled run covering the period 1970–2060.

Results from the two climate simulations have been compared with a RACMO2-LOTOS-EUROS (RLE) simulation forced by the ERA-Interim reanalysis for the period 1989–2009. Both RLE_ECHAM and RLE_MIROC showed considerable deviations from RLE_ERA for daily maximum temperature, precipitation and wind speed. Moreover, sign and magnitude of these deviations depended on the region. The differences in average present-day concentrations between the simulations were equal to (RLE_MIROC) or even larger than (RLE_ECHAM) the differences in concentrations between present-day and future climate (2041–2060). The climate simulations agreed on a future increase in average summer ozone daily maximum concentrations of 5–10 $\mu g\,m^{-3}$ in parts of Southern Europe and a smaller increase in Western and Central Europe. Annual average PM_{10} concentrations increased 0.5–1.0 $\mu g\,m^{-3}$ in North-West Europe and the Po Valley, but these numbers are rather uncertain: overall, changes for PM_{10} were small, both positive and negative changes were found, and for many locations the two climate runs did not agree on the sign of the change. This illustrates that results from individual climate runs can at best indicate tendencies and should therefore be interpreted with great care.

1 Introduction

Ozone and particulate matter (PM) have an adverse impact on the health of human beings and other organisms. They also play a role in the climate system by their interaction with radiation and/or clouds (Raes et al., 2010; Zhang et al., 2010). The day-to-day and even sub-daily variability of concentrations strongly depends on atmospheric conditions, since these govern transport, dilution and deposition, as well as chemical conversions (cloud processes, photochemistry). There is a strong correlation between ozone concentrations and temperature. The correlation of particulate matter with meteorological parameters is more complex and depends on the component (e.g. Tai et al., 2010; Jimenez-Guerrero et al., 2011; Manders et al., 2011, Mues et al., 2012). Due to changes in meteorology associated with a changing climate, ambient concentrations are expected to change even if anthropogenic emissions are kept constant. The quantification of expected changes in concentrations is highly relevant for policy making, as there are strict regulations for concentrations (e.g. EU, 2008; US EPA NAAQS, 2012). Additional emission reductions may be needed to comply with

regulations under expected warmer conditions and changes in other meteorological fields that influence air pollution (e.g. longer stagnant episodes).

A common approach to study the impact of climate change on air quality is to directly use output of climate models in an air quality model (one-way coupling), with many examples for different meteorological models coupled to different air quality models, both at the global and the regional scale (e.g. Dentener et al., 2006; Forkel and Knoche, 2007; Giorgi and Meleux, 2007; Andersson, 2009). The overview by Jacob and Winner (2009) shows that the impact of climate change on air quality depends on the time horizon, region and component, and simulations with various models have resulted in both increases and decreases in concentrations. Results generally show an increase in ozone concentration, related to an increase in temperature. The response of PM to changes in meteorology is weaker and less conclusive, with the different model simulations not even resulting in the same sign of the change.

Climate models themselves are subject to considerable uncertainties due to assumptions and parameterizations and simplifications of processes. All climate models, both global and regional, have significant biases, which are different for each model and region (Christensen et al., 2007). They may represent for example too strong or too weak zonal flow. This is why a multi-model approach is crucial, and this approach is taken by IPCC. Despite the regional differences, there is a general consensus that there is global warming, with very likely an increase in frequency of hot extremes, heat waves and heavy precipitation and a poleward shift of extratropical storm tracks with consequent changes in wind, precipitation and temperature patterns (IPCC, 2007).

So far, the impact of biases in climate models on the outcomes of air quality modeling has not received much attention, and authors have based their estimates of the impact of climate change on air quality on simulation with a single model (e.g. Giorgi and Meleux, 2007; Andersson, 2009; Carvalho et al., 2010). A commonly applied assumption is that a climate model exhibits the same bias structure in both the present-day and the future climate simulation, so that concentration differences can be identified and interpreted straightforwardly. Most one-way coupled simulations only used one realization of the future climate, or two scenarios using the same climate model. But using two scenarios with the same climate model results in a change in amplitude of the change rather than shifts in patterns (Mitchell et al., 1999). Alternatively, Liao et al. (2007) produced a high and a low extreme of a meteorological baseline scenario, based on uncertainty estimates for the individual variables for future climate in terms of their probabilistic distributions. When results from an individual climate model are used, e.g. for flood predictions, bias-corrected precipitation fields are made prior to the application. However, it is very difficult to make *consistent* bias corrections for all meteorological fields at once, which would be required for use in air quality models.

To bypass the use of climate models, an extremely warm summer episode in the present-day climate can be investigated as being representative for an average future summer (Vautard et al., 2007a; Mues et al., 2012). This has the advantage that one can verify the ability of models to represent such conditions with observations (Mues et al., 2012), but in this way it is difficult to look into the variability of the future climate and obtain statistics about extremes. Another way is to directly manipulate the output of a meteorological model to represent expected warmer future conditions (e.g. Im et al., 2011, 2012) and use that as input for the air quality model. The drawback of the latter method is that temperature, precipitation and wind are often modified independently and not in a dynamically consistent way. Therefore, these sensitivity studies can at most be used to identify the most relevant meteorological parameters for air quality, and indicate the possible change due to the change in this meteorological parameter. Since changes due to changes in e.g. temperature, wind and precipitation separately do not simply add up it is only possible to arrive at qualitative results.

Owing to regional biases in global climate models and nonlinear responses of air quality to simulated climate change, results may strongly depend on which climate model is used. The present study aims to provide more insight in this dependency. This is done by using a one-way coupled system consisting of the regional chemistry transport model LOTOS-EUROS and the regional climate model RACMO2. A simulation driven by meteorology from ERA-Interim reanalysis at the boundaries is regarded as reference, best representing the present-day climate. In Manders et al. (2011), the coupled system was compared with LOTOS-EUROS using ECMWF analysis meteorology and observations of concentrations, justifying this approach. Within the EU-Ensembles project RACMO2 participated in an evaluation study in which model output of 16 regional climate models (RCMs) driven by ERA-40 reanalyses was compared with high-resolution daily temperature and precipitation observations in Europe (Kjellström et al., 2010). More recently, RACMO2 simulations forced with ERA-Interim fields have been evaluated with the same set of observations (van Meijgaard et al., 2012). Both studies show that RACMO2 is capable of realistically downscaling re-analyzed meteorology at the 50-km scale, however one should remain aware that local meteorological parameters like wind speed and precipitation derived from (re)analyses should not be used as a substitute for observations. LOTOS-EUROS has been compared with observations for ozone (Curier et al., 2012) and PM (Manders et al., 2009; Mues et al., 2012). In the latter two studies also the dependency of concentration on meteorology has been studied explicitly, showing good general trends but also shortcomings due to species that are not taken into account and flaws in the emissions. Model intercomparison studies (e.g. Vautard et al., 2007b; van Loon 2007; Solazzo et al., 2012) indicate that LOTOS-EUROS is performing very comparable to other models. Since the general performances of

RACMO2 and LOTOS-EUROS separately are assessed comprehensively in the literature mentioned above, output from the coupled system forced with reanalyses will be not compared with observations, but is regarded as the reference in the present article.

Two transient climate runs for the period 1970–2060 have been carried out with the coupled system RACMO2-LOTOS-EUROS. They were driven by boundary conditions from two different GCMs, i.e. ECHAM5 (Roeckner et al., 2003; Jungclaus et al., 2006), henceforth referred to as ECHAM5, and MIROC3.2-hires (K-1 Model Developers, 2004), hereafter referred to as MIROC. Results were complemented by a present-day climate simulation for the period 1989–2009 forced by reanalysis data from ERA-Interim (Dee et al., 2011). Van Ulden and Van Oldenborgh (2006) found that while ECHAM5 and MIROC were both among the five best performing climate models in representing present-day climate conditions in Central Europe, their behavior differs both in terms of zonal mean flow for present-day conditions and in climate change response, which has a strong impact on temperature and precipitation and changes therein.

This study is limited to examining the impact of meteorology only, without feedback mechanisms. Therefore, constant anthropogenic emissions were used in LOTOS-EUROS. However, the impact of meteorology on biogenic and sea salt emissions is included. The presented results are confined to the analysis of long-term average ozone and PM_{10} concentrations over the European modeling domain, and the present and future relationships between concentrations and temperature. Model output from RACMO2 and LOTOS-EUROS is compared for two 20-yr periods, centered around 2000 and 2050, representing time slices of present-day and future climate conditions.

2 Description of models and method

2.1 RACMO2

RACMO2 is the regional atmospheric climate model of KNMI (Lenderink et al., 2003; Van Meijgaard et al., 2008). The RACMO 2.2 version used for this study consists of the 31r1 cycle of the ECMWF physics package embedded in the semi-Lagrangian dynamical kernel of the numerical weather prediction model HIRLAM (Undén et al., 2002) and a few routines to link the dynamics and physics parts. It has participated in ensemble studies with other regional climate models (Jacob et al., 2007; Christensen and Christensen, 2007), which showed that the regional models did reproduce the large-scale circulation of the global driving model, albeit with biases, and that RACMO2 was not one of the extreme models.

RACMO2 employs a rotated longitude-latitude grid to ensure that the distance between neighboring grid points is more or less the same across the entire domain. For the coupled run a RACMO2 domain was configured just encompassing the standard LOTOS-EUROS domain (see Fig. 1). It has a horizontal resolution of 0.44° with 114 points distributed from 25.04° W to 24.68° E longitude and 100 points from 11.78° S to 31.78° N latitude in the rotated grid. The South Pole is rotated to 47° S and 15° E. In the vertical, 40 pressure levels were used. At this resolution RACMO2 uses a model time step of 15 min and output for coupling with LOTOS-EUROS was generated every three hours. The analysis of atmospheric parameters is limited to the interior of the RACMO2 domain, here obtained by omitting an 8-point wide boundary zone.

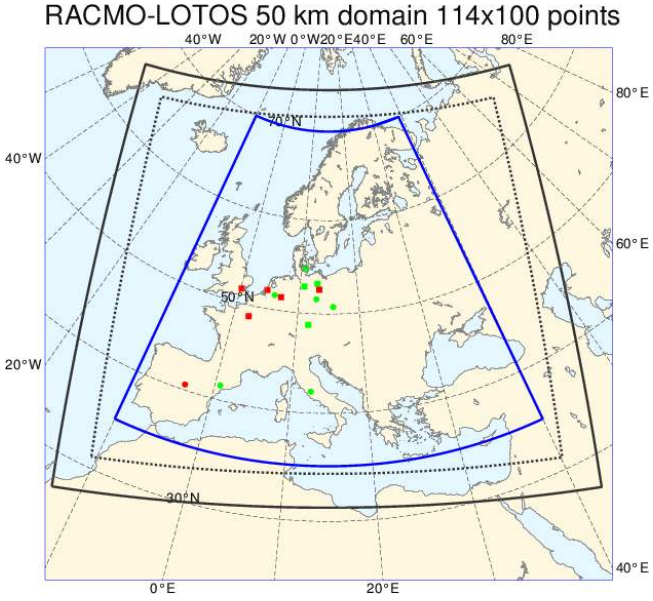

Fig. 1. RACMO domain in black, inner domain dashed, encompassing the LOTOS-EUROS domain (in blue). Points indicate locations that are used in the analyses: red markers indicate cities, green EMEP background locations.

2.2 LOTOS-EUROS

LOTOS-EUROS is a Eulerian chemistry transport model on the European domain (Schaap et al., 2008). It has participated in model intercomparison studies (Vautard et al., 2007b, Van Loon et al., 2007; Solazzo et al., 2012) and is well evaluated for PM_{10} in the Netherlands (Manders et al., 2009). It is used for the daily air quality forecast in the Netherlands and part of the MACC ensemble (http://www.gmes-atmosphere.eu/services/raq/). Modeled species are ozone, nitrogen oxides, sulfur dioxide, ammonia, primary $PM_{2.5}$ and black carbon, primary PM_{10} (excluding $PM_{2.5}$ and black carbon), sulfate, nitrate, ammonium and sea salt and species relevant as precursors or reservoir (peroxy-acetylnitrate, volatile organic carbon). Total PM is defined as:

$$PM_{10} = PPM_{25} + PPM_{10}\_coarse + BC + NO_3^- + NH_4^+ + SO_4^{2-} + 3.26 * (Na_{25} + Na_{10}\_coarse).$$

For (photo)chemical gas reactions a modified CBM IV scheme is used, for secondary inorganic aerosol formation EQSAM (Metzger, 2000) is used.

The regional model is driven by climatological boundary conditions for gases and aerosols. In the present set-up, these boundary conditions were kept constant for consistency, although background concentrations are expected to change. In the present study, anthropogenic emissions for 2005 (MACC 2005 emissions, Kuenen et al., 2011) were used for the whole period to isolate the effect of climate change. Natural emissions of sea salt and isoprene emissions by trees are calculated on-line, as they depend on wind speed (sea salt, Monahan et al., 1986) and temperature (isoprene, Guenther et al., 1993). Dust emissions, forest fire emissions and secondary organic aerosols were not included since they are either too uncertain (secondary organic aerosols), mainly fall outside the domain (dust) or cannot be modeled in a realistic way in a climate run (fire emissions).

The horizontal model domain covered the region 10° W–40° E, 35° N–70° N on a $0.5 \times 0.25°$ regular longitude-latitude grid. In the vertical, five dynamical layers up to 5 km were used, including a static surface layer, and a mixing layer and reservoir layers which vary in time. The horizontal projection of RACMO fields on the LOTOS-EUROS grid was carried out by bi-linear interpolation. The vertical projection of RACMO profiles on the much coarser LOTOS-EUROS vertical grid was achieved by mass-weighted averaging of those RACMO model layers that were contained – fully or partially – in each of the LOTOS-EUROS model layers. Friction velocity and Monin-Obukhov length could be taken from RACMO2 but were recalculated internally in LOTOS-EUROS for consistency with the grid size and land use in LOTOS-EUROS.

For the climate simulations, 3-hourly instantaneous concentrations were stored to reduce the amount of output. Since this may result in missing the daily maximum ozone concentration, this concentration was stored additionally.

2.3 Model runs and analysis method

RACMO2 and LOTOS-EUROS were configured to run side-by-side. Three model runs were performed, with RACMO2 downscaling the following meteorologies:

1. ERA-Interim boundaries, 1 January 1989–31 December 2009,
2. ECHAM5r3 A1B scenario boundaries, transient, 1 January 1970–31 December 2060,
3. MIROC-hires A1B scenario boundaries, transient, 1 January 1970–31 December 2060.

In the text, these runs will be referred to as RLE_ERA, RLE_ECHAM and RLE_MIROC, respectively. Results for the period 1 January 1989 to 31 December 2009 (present-day climate) will be compared to identify biases, and the results for the period 1 January 2041 to 31 December 2060 (future climate) will be compared to the present-day results to study the impact of climate change. Due to the natural variability of the meteorology, it is important to compare long periods. A 20-yr period is chosen to be able to compare with ERA-Interim, although in climate science 30-yr periods are used more commonly.

Exposure to pollutants takes place at ground level. Therefore, this paper considers only ground-level concentrations of ozone and PM_{10}, and their associated meteorology. Climate model output is generally assessed using average temperatures and wind fields. However, these are not the most relevant parameters in studying the impact of climate on ground-level air quality. The following meteorological parameters are considered of particular relevance in relation to air quality:

- Daily maximum surface temperature. High temperatures coincide with high ozone concentrations and both high and low temperatures are often related to stagnant conditions. In particular the number of summer days ($T_{max} > 25\,°C$) is used. For some regions low daily maximum temperatures ($T_{max} < 5\,°C$) are related to stagnant conditions in winter.
- Daily average surface wind speed. Low wind speed is related to stagnant conditions, in particular the number of calm days (daily average wind speed $< 2\,m\,s^{-1}$).
- Rain. Rain is related to wash-out of species, in particular the number of wet days. Since wet deposition is a very efficient removal process, the mere occurrence of precipitation is more important than its intensity and duration. To account for unphysical small amounts of drizzle that often occur in climate models, a threshold of 0.5 mm for daily accumulated rain was set.

These meteorological variables are not independent. For example very high and very low daily maximum temperatures are related to low wind speeds and little precipitation on most locations. In addition, working with threshold values can exaggerate differences when there are many days with values around this threshold. Mixing height is an important variable for PM, and is determined by both temperature (convection) and wind (turbulence). In our analysis, it is represented indirectly by the temperature and wind speed.

To analyze long periods, long-term average values and their standard deviations were calculated for surface temperature, surface wind speed, rain and surface PM concentrations. For surface ozone concentrations, the average daily maximum in summer (June, July, August) was calculated. Spatial patterns were investigated, as well as temporal variability at 15 locations (Fig. 1, Table 1). These locations are a

selection of major European cities and background locations (EMEP stations). The concentrations at the background locations will be representative for a relatively large area, however, for the cities they will only be an indication of the local behavior due to the higher concentrations in these areas with high emissions. Results will be illustrated for the locations Vredepeel and Madrid, which have the most contrasting signature in terms of meteorology and air quality. Vredepeel is situated in a rural area in the south-east of the Netherlands, but may be affected by the densely populated Randstad and nearby Ruhr area, and by local farming (in particular ammonia emissions). Its climate is moderate and affected by the sea. In contrast, Madrid is major city, situated in the central highlands in a much warmer and dryer climate. The model system is not able to resolve cities in detail, but since the emissions are high in these areas the concentrations in the model results are clearly elevated. For this reason cities are included in the analysis. For ozone and PM_{10} the presence of local emission sources can lead to stronger gradients, and Vredepeel has relatively high concentrations for a rural location. Differences in behavior between these two and other analyzed locations will be described qualitatively. For Madrid, Vredepeel and five additional locations, results are presented in more detail. In the Supplement tables with statistics can be found for these locations. In addition to the time averaged values, average relationships between temperature and rain, temperature and wind, temperature and ozone, and temperature and PM_{10} concentrations have been studied for the time series at these stations to study whether these relationships differ between the forcing GCMs and whether they are affected by climate change. For this purpose, all daily values per station were sorted by daily maximum temperature and subsequently averaged in 50 temperature bins. Since the temperature series differ between model runs and stations, the temperature bins differ as well, but do contain the same amount of data. In addition, histograms (probability density functions) were studied. Examples hereof are shown in the Supplement (Fig. S2).

3 Results: meteorology

The meteorological parameters from RLE_ERA, RLE_ECHAM and RLE_MIROC were compared with each other. For the climate simulations, good day-to-day correlations between temperature, wind and precipitation from RLE_ERA on the one hand and RLE_ECHAM or RLE_MIROC on the other hand cannot be expected. However, for the present-day climate, at least the frequency of occurrence of events and their amplitude should be similar. The mean sea level pressure is an indication of the general circulation and will be discussed first. Then the number of warm days, wet days and calm days will be compared to establish projected shifts in the more extreme conditions. In addition, the average annual cycle for temperature, rain and wind speed was studied for a number of stations. In the Supplement, the statistics for a selection of locations is summarized.

Table 1. Location of stations for detailed analysis (see also Fig. 1).

Country	station	lon	lat
Denmark	Keldsnor	10.73	54.72
France	Paris	2.35	48.85
Germany	Berlin	13.34	52.54
	Essen	6.96	51.40
	Melpitz	12.92	51.52
	Neuglobsow	13.03	53.14
	Neustadt (Donau)	11.77	48.81
	Waldhof	10.75	52.80
Italy	Montelibretti	12.63	42.10
Netherlands	Vredepeel	5.85	51.53
	Rotterdam	4.48	51.93
Poland	Sniezka	15.73	50.73
Spain	Els Torms	0.71	41.40
	Madrid	−3.70	40.41
United Kindom	London	0.16	51.50

3.1 General circulation

A first indication of the ability to represent the circulation properly can be derived from the average patterns of mean sea level pressure (mslp). As shown in Fig. 2a, the centers of low pressure during winter in both RLE_ECHAM and RLE_MIROC have shifted to the south compared to RLE_ERA, resulting in a more southerly average position of the Atlantic storm track. In RLE_ECHAM, this shift extends to the whole of Western Europe giving rise to a stronger zonal circulation in this region compared to RLE_ERA. In RLE_MIROC, on the other hand, the center of low pressure is positioned much more to the west over the Central Atlantic which weakens its influence over the European landmass, increasing the likelihood of stagnant conditions over the continent. Figure 2b shows that all simulations feature a prominent Azores anticyclone during summer, as expected. In RLE_ECHAM, the pressure over Northern Europe is on average lower than in RLE_ERA giving rise to a more predominant (north) westerly flow over Western Europe than in RLE_ERA and very stable conditions over the Mediterranean. RLE_MIROC, on the other hand, simulates a higher mslp over Scandinavia and the North-East Atlantic than RLE_ERA which weakens the north-south pressure gradient and reduces the oceanic influence of the weather over the continent. This results in more stable summertime conditions in Northern Europe and relatively more unsettled conditions in Southern Europe as compared to RLE_ERA. Thus, in general, the circulation structures of RLE_ECHAM and RLE_MIROC have mutually different characteristics, and they also differ from those of RLE_ERA. Furthermore, the

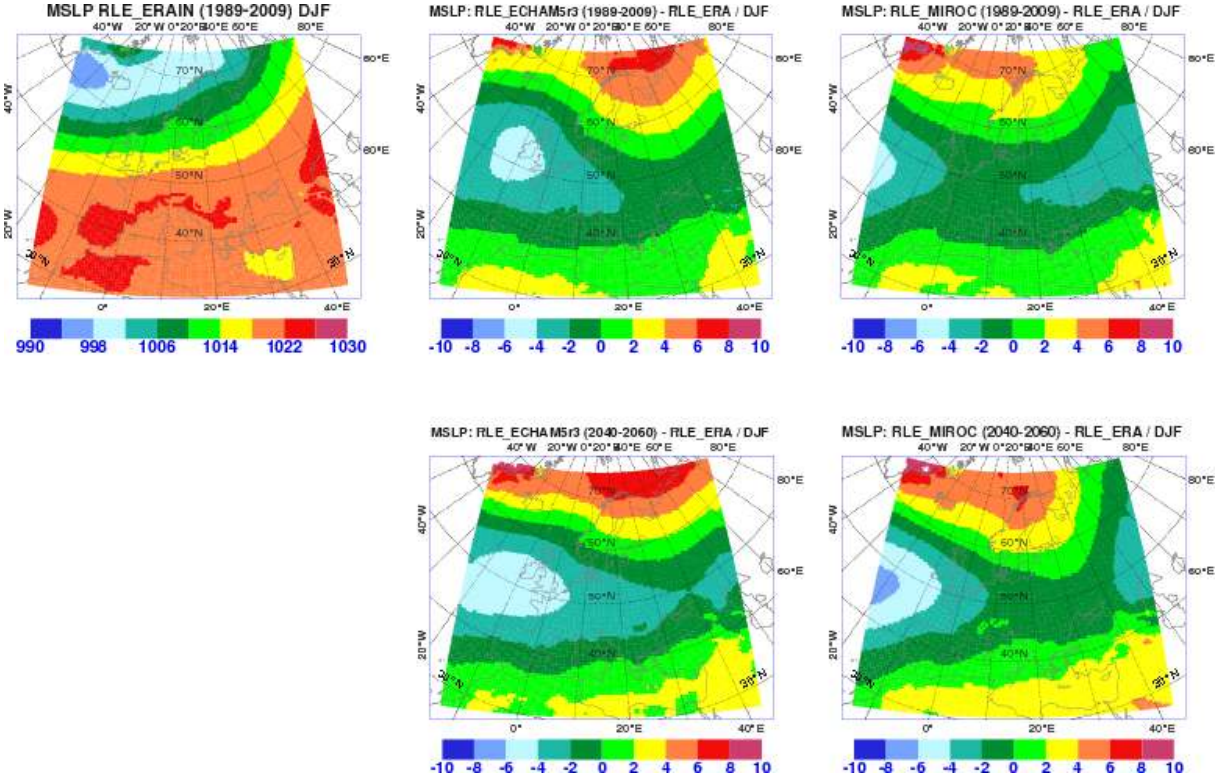

(a)

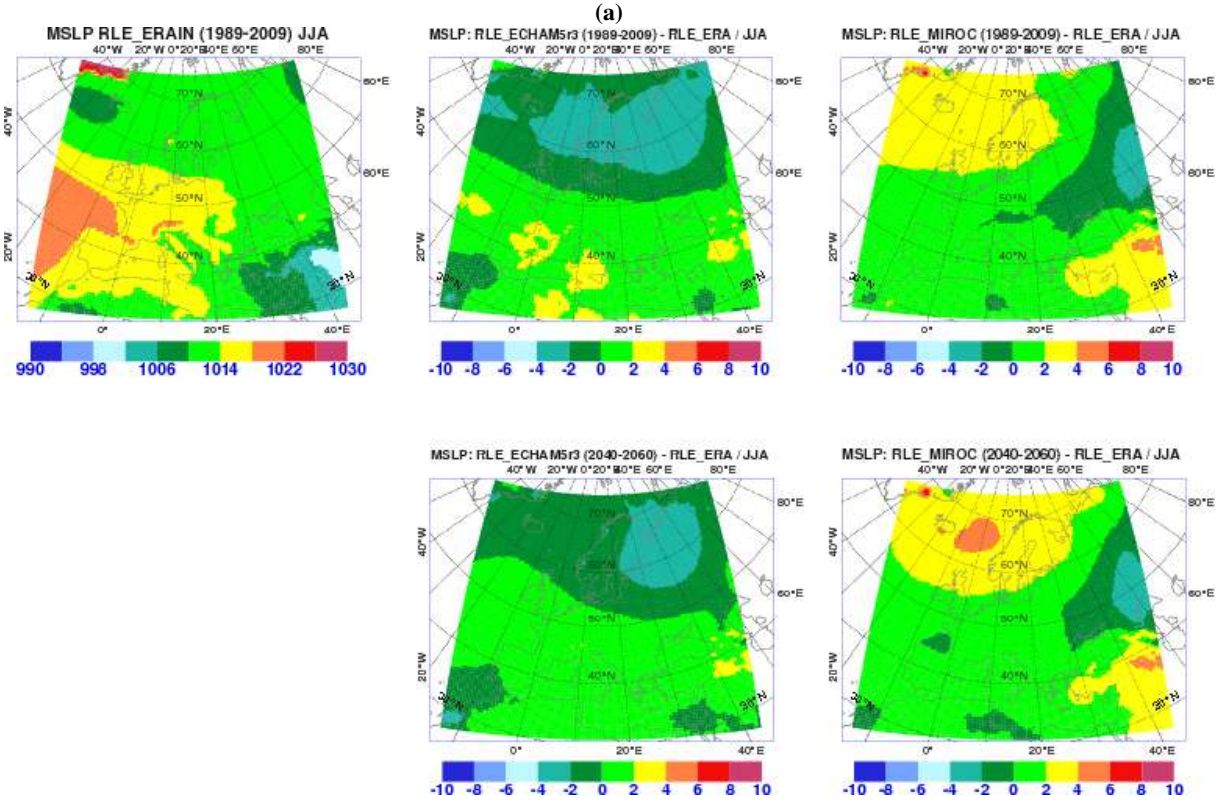

(b)

Fig. 2. (a) Top-left panel: average winter (December-January-February) mean sea level pressure (hPa) from RLE_ERA. Central (right-hand) panel: differences in mslp between RLE_ECHAM5 (RLE_MIROC) and RLE_ERA for the present-day climate (1989–2009, top row) and the future climate (2040–2060, bottom row). **(b)** Like **(a)** but for summer (June-July-August).

differences between future climate and present-day climate within each of the transient runs are much smaller than the differences between the models. The impact of these general findings on near-surface temperature and wind speed and on precipitation will now be discussed for the present-day and future climate.

3.2 Temperature

For most areas, the average daily maximum temperatures in summer for the present-day climate from RLE_ECHAM are up to 3 °C lower (e.g. Vredepeel) than those from RLE_ERA, and also the number of days with $T_{max} > 25$ °C is much lower (Figs. 3, S1, S2 and Table S1a). Differences in annual average daily maximum temperatures between RLE_ECHAM and RLE_ERA are smaller than the interannual variability observed in RLE_ERA. The differences are larger for the summer period, with the exception of the Spanish locations. In general the differences are significant at the 0.05 level, except for the analyzed locations Els Torms (annual mean) and Madrid (summer mean). In between periods 2000 and 2050, the increase in annual average daily maximum temperature is larger than the interannual variability of this parameter, but for the summer period the increase is of the same order of magnitude as the interannual variability. Both differences are significant at all stations. For North-West Europe, RLE_ECHAM future climate summer temperatures are close to the present-day RLE_ERA summer temperatures. Furthermore, the seasonal cycle is weaker: the difference between summer and winter temperatures is smaller than for RLE_ERA (Fig. 4). For Spain, the RLE_ECHAM present-day climate temperatures resemble those of RLE_ERA more closely and the RLE_ECHAM future climate simulation gives the highest temperatures.

The difference in annual mean and summer mean daily maximum temperature between RLE_MIROC and RLE_ERA is smaller than the interannual variability, with the exception of the Spanish stations (Fig. S1). Differences are found significant for all analyzed locations, except for Sniezka, Montelibretti, Paris and Neustadt. The difference between future and present-day annual and summer average daily maximum temperature is larger than the interannual variability for all stations and is significant. Temperatures from RLE_MIROC correspond better to the RLE_ERA's present-day summer and summer-winter difference than RLE_ECHAM. However, RLE_MIROC tends to be somewhat warmer than RLE_ERA (2 °C) in early summer for North-West Europe. Also in the future climate RLE_MIROC gives a 2 °C higher average summer daily maximum temperature than RLE_ECHAM. However, for Southern Europe RLE_MIROC tends to be the coldest model. In Spain, for example, RLE_MIROC clearly simulates the lowest temperatures in present-day summer, whereas in the future climate the temperatures from RLE_MIROC and RLE_ECHAM become comparable in summer, autumn and early winter. In future late winter/early spring, RLE_ MIROC is warmer than RLE_ECHAM. This is also reflected in Fig. 3, which shows that RLE_ ERA yields more warm days than RLE_ECHAM in a broad region around 50° N, the Sahara and the Mediterranean, whereas RLE_MIROC is comparable to the run using RLE_ERA in North-West Europe, is much warmer than RLE_ERA in Russia and parts over the Mediterranean Sea, while it is much colder than RLE_ERA in the Mediterranean countries. For the future climate, both simulations show an increase in summer days with a clear north-south gradient, but the changes are much larger for RLE_MIROC than for RLE_ECHAM. Figure S2 clearly illustrates the contrasting behavior of the two simulations for Vredepeel and Madrid, showing differences in both the shape of the distribution and the position of the maximum.

3.3 Precipitation

RLE_ECHAM and RLE_MIROC both produce more precipitation than RLE_ERA, with RLE_ECHAM being the wettest almost everywhere (Table S1b). RLE_ECHAM simulates a larger number of wet days in Western Europe than RLE_ERA, but it has less wet days near Norway and the Eastern Mediterranean and around the Black Sea (Fig. 5, Table S1b). For RLE_MIROC however, the number of wet days in Northern Europe, north of 50° N, is smaller than for RLE_ERA, while it is larger south of this latitude. The difference between future and present-day climate is comparable for the two transient runs, with in the future less precipitation in the Mediterranean area and somewhat more in Central and Northern Europe, with a slightly stronger signal for RLE_MIROC in the Mediterranean. The annual cycle of monthly mean precipitation (Fig. 4) shows the same general pattern for several model runs and time windows. For most locations in North-West Europe (e.g. Vredepeel), the amount of precipitation is relatively constant throughout the year. RLE_ECHAM clearly is the wettest model, with little difference between present-day simulations for the first half of the year and larger differences in the second half. RLE_MIROC is close to RLE_ERA for the present-day climate, except for late summer when it is wetter. For the future climate, RLE_MIROC becomes wetter, except for the late summer period. So in a future climate both transient runs generate a wetter spring/early summer and little change in autumn. In South-West Europe, there are regional differences. For Madrid and Montelibretti, there is a clear annual cycle, with dry summer months and a wet winter. RLE_ECHAM 2041–2060 is the most extreme case, with ca. 100 mm more rain in January than in June. RLE_MIROC 1989-2009 shows less variation during the year. In contrast, for Els Torms precipitation is relatively constant throughout the year with a small summer minimum in the RLE_ERA and RLE_ECHAM runs, and a summer maximum in RLE_MIROC.

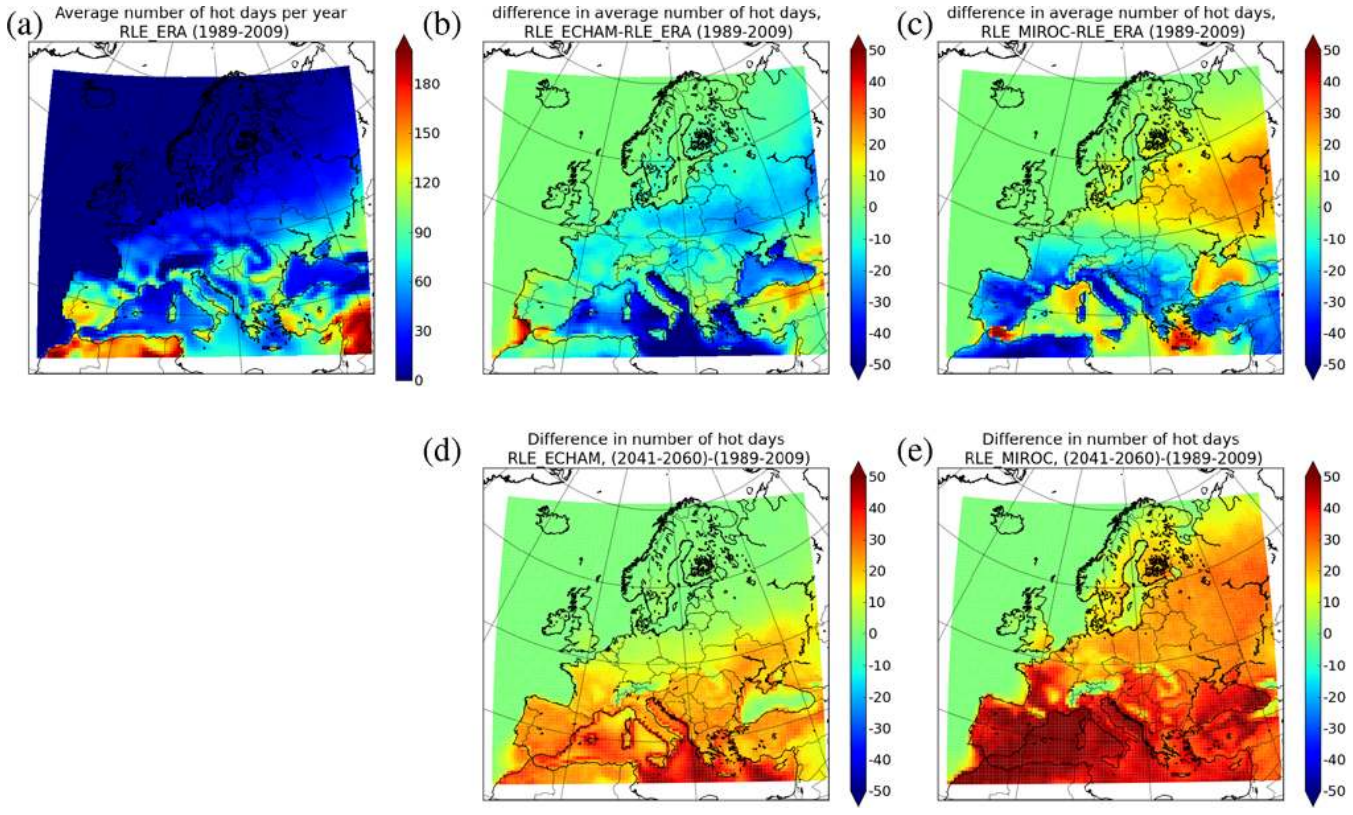

Fig. 3. Average number of summer days ($T_{max} > 25\,°C$). **(a)** Present-day RLE_ERA, **(b)** difference present-day RLE_ECHAM and RLE_ERA, **(c)** difference present-day RLE_MIROC and RLE_ERA, **(d)** difference future climate and present-day climate RLE_ECHAM, and **(e)** difference future climate and present-day climate RLE_MIROC.

3.4 Wind speed

According to the model, 10-m wind speed in mountainous regions is in general lower than in flat areas at lower elevations. This is clearly illustrated by the spatial distribution of the annual mean number of calm days for RLE_ERA in Fig. 6. This behavior is caused by the high value of surface roughness length for momentum associated with mountainous terrain. While the contrast in number of calm days between flat and mountainous areas might not be confirmed by observations we want to emphasize that this study deals with differences or changes in parameters, and not with their absolute values. All 10-m wind speed output has been obtained with the same surface roughness map which considerably helps in the interpretation of the relative differences.

For the present-day climate, the number of calm days for RLE_ECHAM is comparable to that for RLE_ERA in Northern Europe, however, in Central and Southern Europe, and at the eastern boundary of the domain RLE_ECHAM predicts less calm days than RLE_ERA (Fig. 6). RLE_MIROC tends to simulate more calm days than RLE_ERA, except in North-West Africa and at the eastern boundary of the domain. The difference between future and present-day climate is small in both transient simulations: less than 10 days on average in the RLE_ECHAM run, and slightly more for RLE_MIROC, which predicts there will be more calm days in larger areas in the future climate, although there are local exceptions. The annual cycles of wind speeds are similar for all runs and periods (Fig. 4). For North-West Europe (e.g. Vredepeel), RLE_ERA is in between RLE_ECHAM (more wind) and RLE_MIROC (less wind). The largest differences occur in summer which is the period with lowest wind speed (Fig. 4). Furthermore, in Vredepeel, also the differences between the present-day and future climate time series are small. For Southwestern Europe (e.g. Madrid, Els Torms), wind speeds tend to be lower, and are nearly constant throughout the year for RLE_ERA except for a weak late winter/spring maximum. The transient simulations show a stronger annual cycle, with more wind in (late) winter/early spring than RLE_ERA but in summer their wind speeds are close to those of RLE_ERA. RLE_ECHAM deviates most from RLE_ERA. Again, the difference between present-day and future average wind speed is very small in both transient simulations. For other locations in South Europe (Montelibretti) the behavior is similar, with a slightly stronger annual cycle.

For all investigated meteorological parameters, the observed differences are not just shifts in amplitude, but also

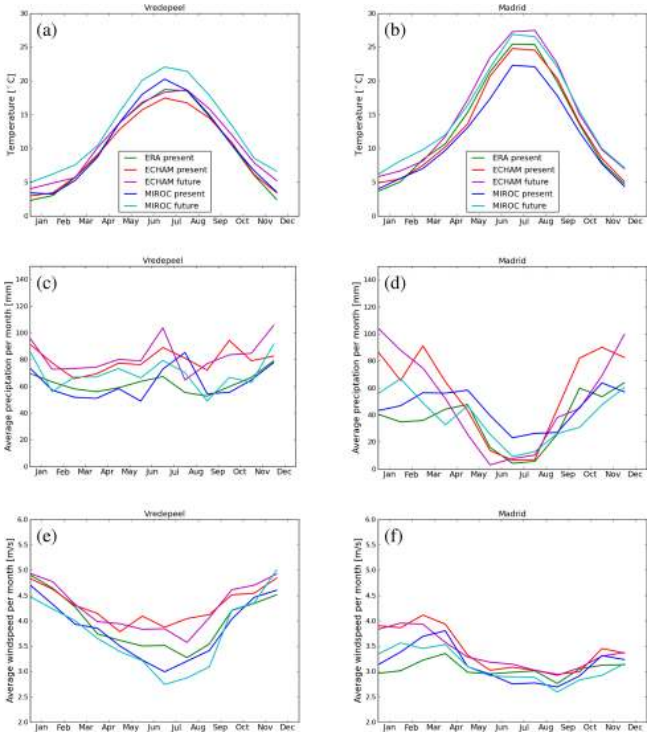

Fig. 4. Average annual cycles of monthly mean values for daily maximum temperature **(a, b)**, monthly mean precipitation **(c, d)** and monthly mean wind speed **(e, f)** at Vredepeel (left) and Madrid (right) derived from various downscaling experiments with RACMO2.

shifts in the spatial patterns. The results are consistent with the conclusions derived from a comparison of global model simulations for present-day climate conditions by Van Ulden and Van Oldenborgh (2006). ECHAM5 predicted less easterly flow than observed for present-day climate, whereas MIROC tended to be more stagnant, which has a direct impact on temperature and rain. The output from two global models was rather consistent concerning the simulated change in annual mean temperature across Europe, but the models differed considerably in seasonality.

4 Results: concentrations of ozone and PM_{10}

4.1 Present-day climate

For ozone, the summer average daily maximum (June-July-August) was studied (Fig. 7a, Fig. S1). RLE_ERA shows a general north-south gradient. Ozone concentrations are highest above the Mediterranean Sea (up to $150\,\mu g\,m^{-3}$), followed by lower concentrations ($110\,\mu g\,m^{-3}$) in industrial areas in southern Europe (Po Valley, around Porto, Rhone delta) and in Central Europe. Figure 7b shows that PM_{10} concentrations are highest in densely populated and industrialized areas (The Netherlands, Ruhr area, Po Valley, Poland and major cities) and above the sea, due to the high local contribution of sea salt. Lowest concentrations are found above Scandinavia, Eastern Europe, Balkan, Ireland, Scotland, parts of Spain and Northern Africa. The low concentrations are partly unrealistic, since no dust and secondary organic aerosol (SOA) was taken into account. SOA may contribute significantly to PM in large parts of Europe (e.g. Gelencsér et al., 2007; Bergström et al., 2012), depending on anthropogenic and biogenic emissions and on the oxidative capacity of the atmosphere. Saharan dust mainly affects the Mediterranean area.

For the present-day climate, summer ozone concentrations in the RLE_ECHAM run are up to $12\,\mu g\,m^{-3}$ lower than in the RLE_ERA run in a large part of the domain (Fig. 8a, Fig. S1), in particular in North-West Europe, the Baltic Sea region and the Mediterranean area. Only in a few small areas at the southern boundary of the domain, RLE_ECHAM yields higher concentrations than RLE_ERA. For RLE_MIROC it is the other way around, with concentrations of up to $12\,\mu g\,m^{-3}$ higher in North-West Europe and some areas around the Mediterranean Sea. The differences in ozone concentration between the present-day transient runs and RLE_ERA are not clearly correlated with the spatial pattern of the ozone concentration from RLE_ERA, indicating a shift in patterns rather than just differences in amplitude. This is consistent with the notion that changes in meteorological conditions can (in part) be associated to changes in patterns. The difference in ozone concentration between the transient runs and RLE_ERA can only partly be related to the patterns of number of summer days, since the sensitivity of ozone to temperature depends on the location and the temperature, as will be illustrated further on. Relative differences (not shown) have a spatial pattern that follows the pattern of absolute differences. Over sea, differences with RLE_ERA concentrations are up to 20 % for both RLE_ECHAM and RLE_MIROC, in particular at the ship tracks. Over land, the relative differences are less than 10 %. For RLE_ECHAM, the difference with RLE_ERA is larger than the interannual variability, except for the Spanish locations, and was significant at all analyzed locations. For RLE_MIROC the differences with RLE_ERA tend to be smaller than the interannual variability (Fig. S1), although they were significant at most locations (not significant at Madrid and Montelibretti). The probability distribution function (pdf, Fig. S2) for Vredepeel falls off more steeply for RLE_ECHAM than for RLE_ERA and RLE_MIROC. In addition, concentrations between 100 and $150\,\mu g\,m^{-3}$ occur more often for RLE_MIROC, though for higher concentrations the curves of all three simulations are close together for Vredepeel. This behavior is observed for all stations in North and Central Europe. For Madrid all curves decrease very rapidly for concentrations of more than $80\,\mu g\,m^{-3}$. For Montelibretti and Els Torms the decrease is not as steep but the curves are also closely together for concentrations above $110\,\mu g\,m^{-3}$, albeit with at Els Torms a

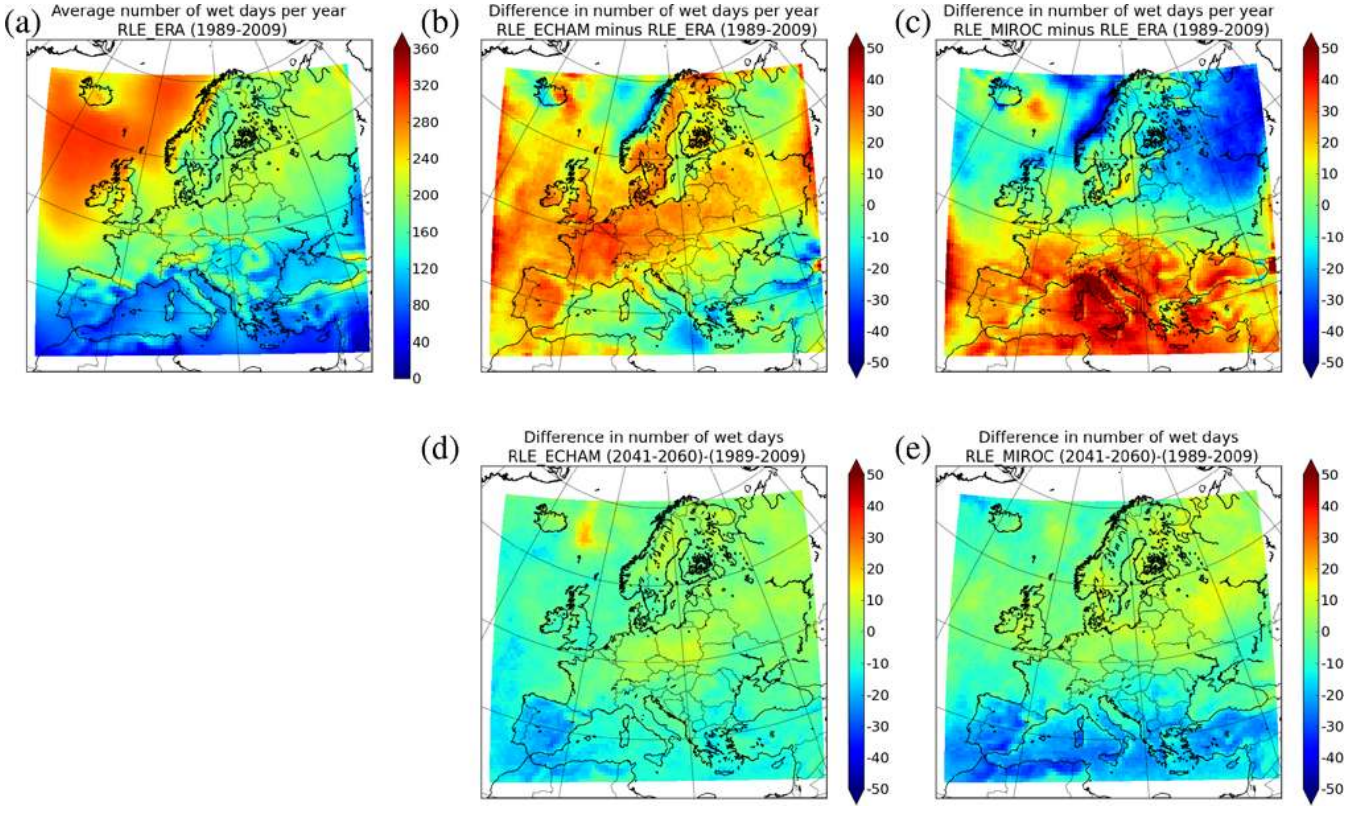

Fig. 5. Like Fig. 3, but showing the average number of wet days.

local maximum just below 100 µg m^{-3} for RLE_ERA and RLE_ECHAM and just above it for RLE_MIROC.

Over land, simulated total PM_{10} concentrations in the present-day part of both transient runs are lower than in the RLE_ERA run. RLE_ECHAM differs much more from RLE_ERA than RLE_MIROC, with the exception of specific locations in Russia (Fig. 9). The spatial pattern of differences in PM_{10} concentrations between RLE_ECHAM and RLE_ERA can be related to the spatial pattern of the (reduced) number of calm days (Fig. 6), reflecting the relationship between high PM concentrations and low wind speed (Manders et al., 2009, 2011), although also precipitation will play a role. For RLE_MIROC, the differences are smaller and the increase in number of wet days may contribute more to the lower PM_{10} concentrations seen in this simulation than the changes in number of calm days. Over sea, the difference in total PM_{10} is particularly large, and can easily be related to wind-generated sea salt. The generation of sea salt aerosol depends strongly on the 10m wind speed (Monahan et al., 1986). Above the Northern seas, RLE_MIROC tends to have lower wind speeds (not shown) than RLE_ERA and RLE_ECHAM, leading to reduced sea salt emissions. In the Mediterranean area, the wind speed tends to be lower in RLE_ERA than in RLE_ECHAM and RLE_MIROC (less calm days, Fig. 6, wind speeds for Els Torms, Table S1c), leading to more sea salt generation in the latter simulations. In RLE_ECHAM this effect is reinforced by a decrease in number of wet days, leading to less wet deposition, whereas in RLE_MIROC the increase in precipitation partly counterbalances the increase in sea salt aerosol production so that the concentration differences with RLE_ERA are smaller for RLE_MIROC than for RLE_ECHAM. Relative differences between the transient runs and RLE_ERA (not shown) of up to 25 % are found. The relative differences follow the spatial patterns of the absolute differences, except for Scandinavia where very low PM concentrations and large relative differences are found. The differences between RLE_ERA and RLE_ECHAM are equal to or larger than the interannual variability, while for RLE_MIROC the differences are smaller than the interannual variability (Fig. S1). For RLE_ECHAM, the differences were significant at nearly all analyzed stations (except for Neuglobsow and Keldsnor), while for RLE_MIROC they were not, except for Madrid, Els Torms and Montelibretti (and Waldhof, Neustadt and Keldsnor). The probability distribution plot of Vredepeel (Fig. S2) is clearly shifted towards the lower concentrations for RLE_ECHAM when compared with RLE_ERA and RLE_MIROC. For most other rural stations the differences between the models are very small and the pdf was narrow, reflecting the low concentrations except for Keldsnor which showed two maxima. For Madrid, RLE_ECHAM has a pdf with a maximum at 12 µg m^{-3}, i.e.

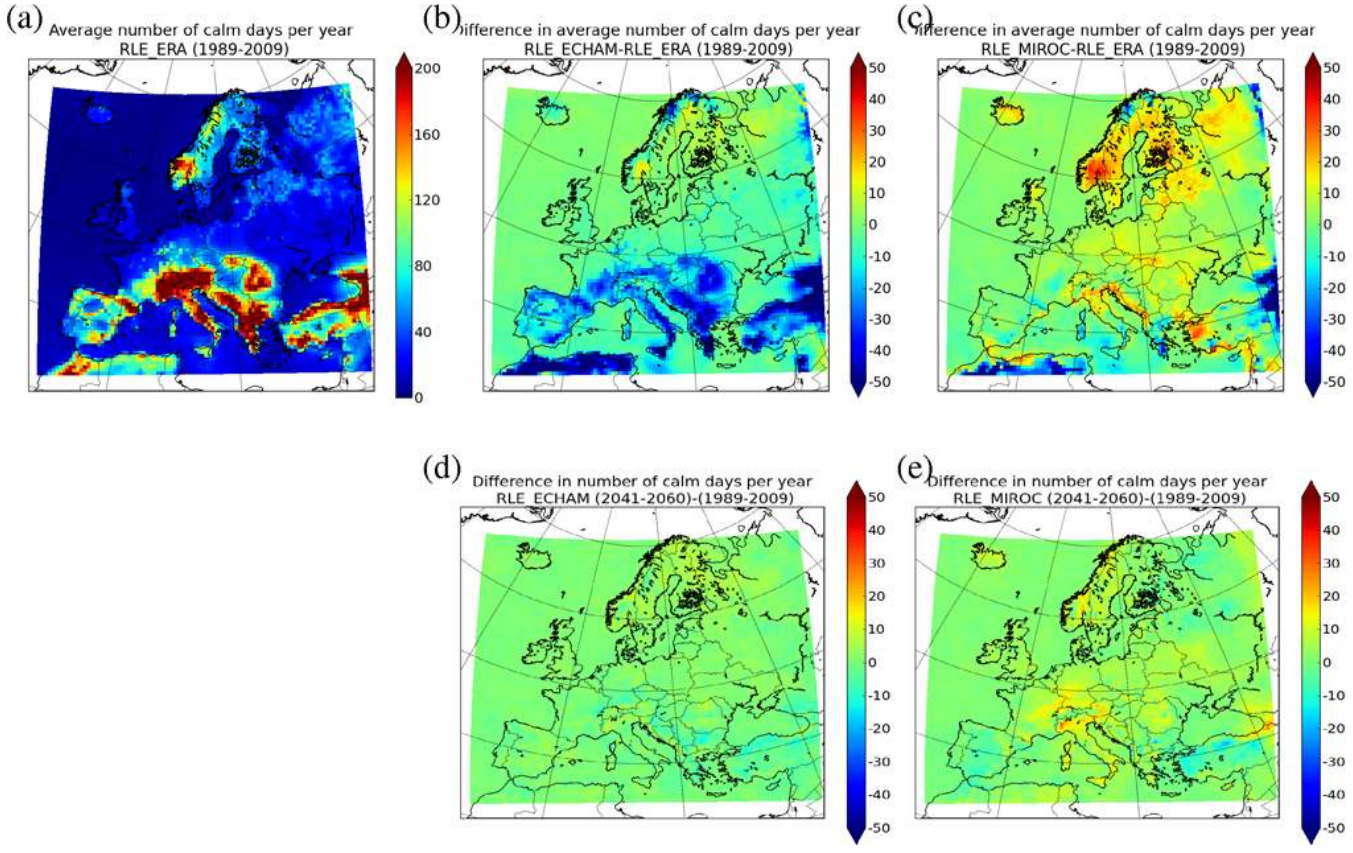

Fig. 6. Like Fig. 3, but showing the average number of calm days.

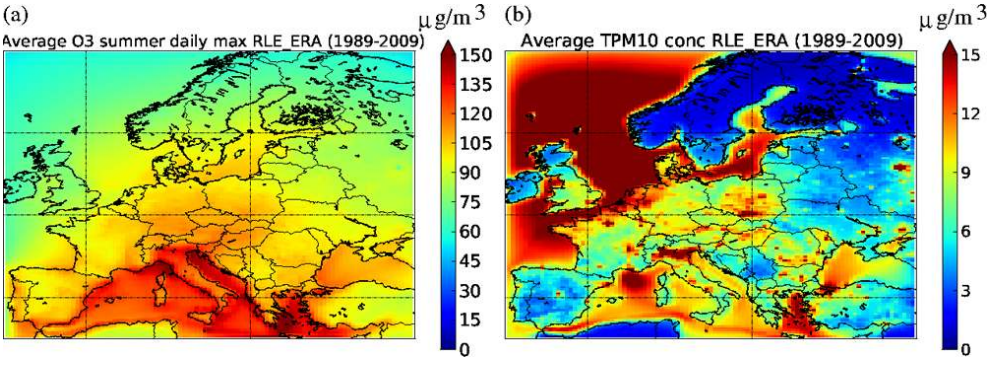

Fig. 7. Average O_3 daily maximum concentrations (June-July-August) **(a)** and annual average total PM_{10} concentration **(b)** obtained with RLE_ERA (1989–2009).

at lower concentrations than RLE_ERA and RLE_MIROC, and without the second maximum at $22\,\mu g\,m^{-3}$ displayed by RLE_ERA and RLE_MIROC. For Els Torms, the pdfs of RLE_ECHAM and RLE_ERA are shifted towards slightly lower concentrations compared to the pdf of RLE_ERA. For Montelibretti the location of the maximum is the same for the three simulations, but the distribution is much narrower for RLE_ECHAM and wider for RLE_MIROC.

4.2 Concentration changes due to climate change

Both RLE_ECHAM and RLE_MIROC show an increase in average O_3 summer maximum concentrations in the future, with values of up to $12\,\mu g\,m^{-3}$ higher than in the present-day climate (Fig. 8). These differences are found over much larger areas in the RLE_MIROC than in the RLE_ECHAM simulation. This is consistent with Fig. 3, which illustrates that the increase in average maximum

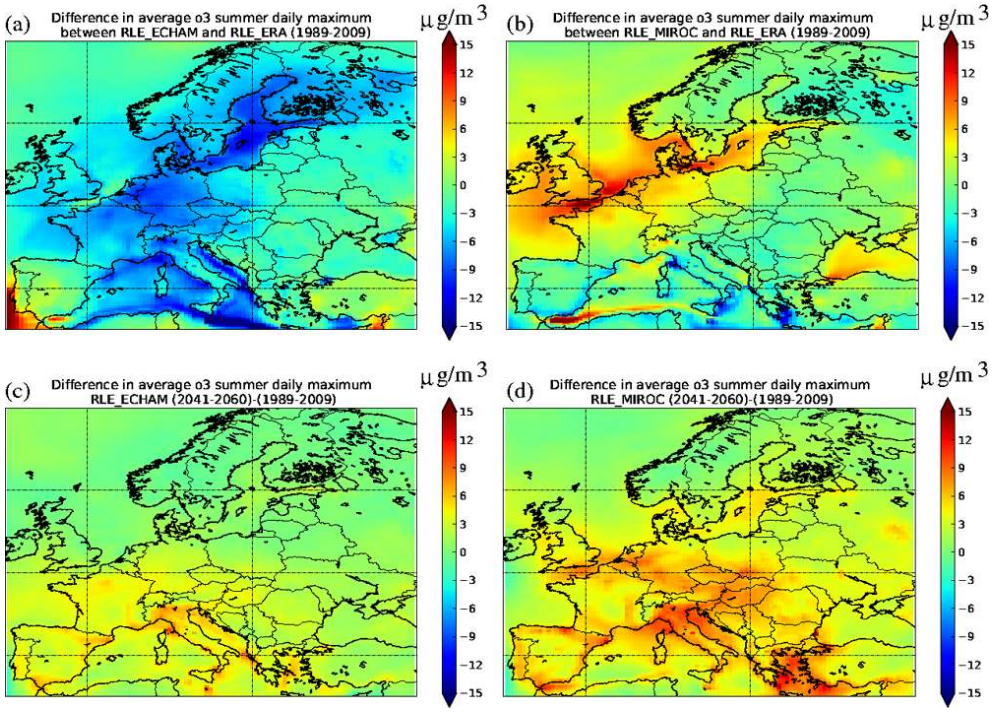

Fig. 8. Differences between 20-yr O_3 average daily maximum concentrations (June-July-August) in $\mu g\,m^{-3}$. Upper panels: **(a)** differences between present-day climate RLE_ECHAM and RLE_ERA and **(b)** between present-day climate RLE_MIROC and RLE_ERA. Lower panels: difference between future climate and present-day climate for **(c)** RLE_ECHAM and **(d)** RLE_MIROC.

temperature is larger and more widespread in RLE_MIROC than in RLE_ECHAM, leading to larger responses in ozone concentration. Moreover, the change in ozone concentration with temperature depends on the region since it is dependent on the availability of NO_x and VOC, so that the same temperature changes may lead to different changes in concentration for different regions. This point is further illustrated in the next section. Relative differences with the present-day climate simulation are up to 5 % for RLE_ECHAM and up to 10 % for RLE_MIROC. Again, the patterns of the relative differences closely follow those of the absolute differences. For RLE_ECHAM, the difference in ozone concentration between future and present-day climate is smaller than the interannual variability in Northern Europe and approximately equal to the interannual variability in Southern Europe. Differences are found significant for most locations in Fig. 1, except for Rotterdam and London and the EMEP locations Neuglobsow and Keldsnor. For RLE_MIROC the difference in ozone concentration induced by climate change is larger than the interannual variability (Fig. S1) and significant for all locations. For both Vredepeel and Madrid, the shift in temperature probability distribution is reflected in the frequency distribution of ozone (Fig. S2), with largest differences between future and present-day climate for RLE_MIROC. In all cases there is a clear extension of the tail of the pdf towards higher concentrations.

Differences in PM_{10} concentrations between future and present-day climate are rather small. For RLE_ECHAM, concentrations are up to $2\,\mu g\,m^{-3}$ lower above the Atlantic, east of Norway, which could be a combined effect of more precipitation in that region in the future climate (more wet deposition) and lower wind speeds (less sea salt generation). Differences over the continent are very small (less than $0.5\,\mu g\,m^{-3}$), except for a small area around Moscow, where concentrations have decreased by more than $2\,\mu g\,m^{-3}$. For the RLE_MIROC run, differences above the continent are somewhat larger but still small: concentrations increase up to $0.7\,\mu g\,m^{-3}$ in the Netherlands and the North-East of Spain, and up to $2\,\mu g\,m^{-3}$ in the Po Valley, while, again, the concentration decreases distinctly around Moscow. Relative differences are less than 10 % for RLE_ECHAM and up to 10 % for RLE_MIROC, with patterns related to the patterns of absolute differences. Only for Scandinavia the small absolute differences still yield large relative differences. For both RLE_ECHAM and RLE_MIROC the changes in PM_{10} concentrations associated with climate change are found smaller than the present-day interannual variability derived for the analyzed locations (Fig. S1). These changes in PM concentration (future-present) are not significant at most analyzed locations, except for Sniezka, Keldsnor, Neuglobsow and Neustadt (RLE_ECHAM) and Vredepeel (RLE_MIROC). For RLE_MIROC, the PM_{10} pdfs at Melpitz, Neuglobsow and Berlin change in shape from a single maximum for the

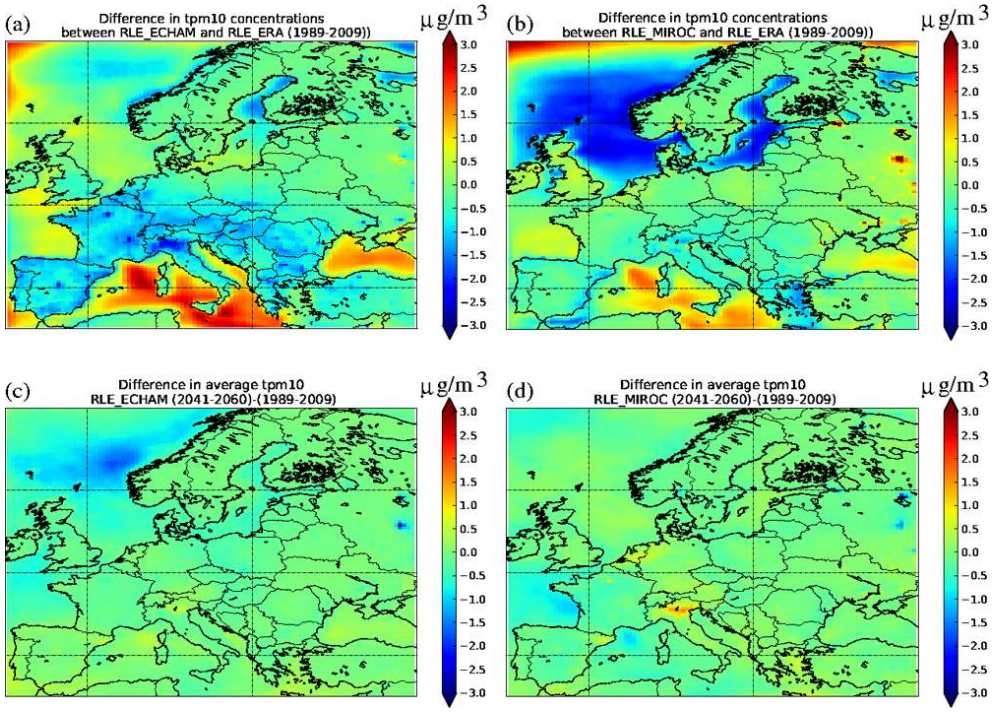

Fig. 9. Like Fig. 8, but showing differences between 20-yr total PM_{10} concentrations.

present-day to two maxima for the future climate (one at lower and one at higher concentrations), while the pdf at Madrid shows the opposite change (from two maxima to a single maximum). For other stations and for RLE_ECHAM, the shape of the pdf and the location of the maximum did not change clearly.

4.3 Changes in average correlations between temperature and ozone or PM_{10} concentrations

The average relationships between ozone or PM_{10} concentrations on the one hand and temperature on the other hand have been investigated for several sites. The results are again illustrated for Vredepeel and Madrid (Fig. 10). For each site the general tendencies are similar for the different model simulations, but there are notable differences between the various sites.

For ozone the relationship with temperature is very distinct and has little scatter. There is a gradual increase with temperature, but the slope is not constant with temperature and differs between locations. For Vredepeel, for example, the slope seems to become somewhat steeper for temperatures above 20 °C, whereas for Madrid the figure shows a leveling-off for temperatures above 20 °C. The value of the slope also differs slightly between model runs. Madrid shows the largest contrast with Vredepeel. The highest ozone concentrations in Madrid are nearly 40 $\mu g\,m^{-3}$ lower than in Vredepeel, in spite of the higher temperatures. The summer average concentrations are highest at Montelibretti, but the maximum

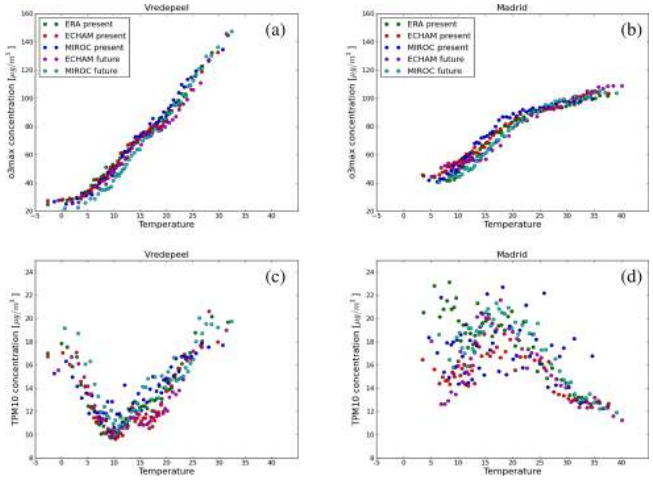

Fig. 10. Average relationship between either **(a, b)** ozone daily maximum or **(c, d)** total PM_{10} from LOTOS-EUROS and daily maximum temperature (°C) for the meteorologies downscaled with RACMO.

ozone concentrations at that site are not higher than those observed at Vredepeel. This does not contradict the general north-south gradient in mean O_3 concentrations with high concentrations in the south, since the high temperatures favoring high ozone concentrations occur more frequently in the south. The leveling-off observed at Madrid is not seen to this extent at the other locations, like Montelibretti or

Paris. The difference in slope between the locations can probably be attributed in part to the local NO_x/VOC ratio. In the Netherlands, NO_x concentrations are generally high and ozone production is assumed to be VOC-limited. Here, increased VOC emissions from trees at higher temperatures accelerate the increase in ozone concentrations, leading to a steeper increase of ozone concentration with temperature. In contrast, on the Iberian Peninsula, the ozone formation is generally assumed to be NO_x-limited, so that the biogenic VOC production at higher temperatures would not lead to additional ozone formation, and here, a deep boundary layer associated to fair weather may result in more dilution. Moreover, for Madrid the local NO_x emissions contribute to the local destruction of ozone (titration).

Total PM_{10} concentrations at Vredepeel show a minimum value around a daily maximum temperature of 10 °C. For Madrid the curve is the other way round: PM_{10} concentrations are highest around 17 °C, with linear decreases for both higher and lower temperatures, except for the coldest days which have relatively high concentrations. In contrast, for Els Torms (not shown) PM_{10} shows little variation with temperature while concentrations are considerably lower. There may be several causes for these differences. First of all, the differences can be caused by the relationships of wind speed and precipitation with temperature at the sites. At Vredepeel, higher wind speeds (mixing) and more precipitation (wet deposition) occur at temperatures around 12 °C, explaining the PM minimum at this temperature. In contrast, for Madrid high wind speeds and precipitation are associated with nearly the lowest temperatures (not shown). The decrease in PM_{10} concentration for higher temperatures is counter-intuitive, since at these temperatures wind speeds and precipitation are generally lower than on average. However, at high temperatures the mixing layer is expected to be deeper, leading to more dilution. The effect may in part be due to the relatively coarse grid resolution, which may result in considerable dilution of the Madrid emissions since it is surrounded by areas with low emissions and concentrations. In this case, the results may strongly depend on the wind direction, which we did not take into account in our analysis since it is a local relationship. An indication for this is the large scatter in PM_{10} for Madrid. Another cause may be the contribution of the different components of PM_{10} (not shown). In Vredepeel, ammonium and nitrate concentrations are higher than at other locations used in the analysis, due to nearby ammonia emissions from intensive farming. There, temperature-dependent reactions involving secondary inorganic aerosol and the volatility of ammonium nitrate may have an impact. In contrast, in Madrid the inert black carbon contributes most to PM_{10} and concentrations are determined more directly by dilution, transport and deposition For other locations the behavior is somewhat in-between the illustrated results, with in general higher PM values for lower temperatures, a minimum for temperatures around 15 °C, however, the increase in PM concentration with temperature at high temperatures

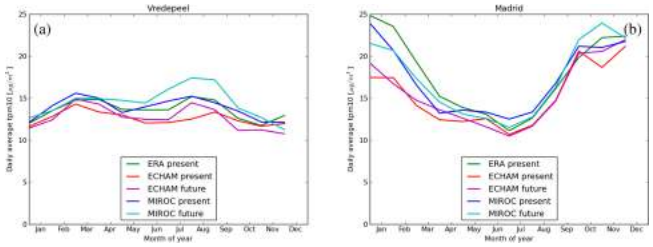

Fig. 11. Simulated daily mean PM_{10} concentrations for Vredepeel **(a)** and Madrid **(b)** averaged over 20 yr.

was not reproduced everywhere. For Els Torms, for example, PM_{10} concentrations vary little with temperature. However, the underlying modeled species at this site do show clear trends with temperature: the ammonium concentration increases with increasing temperature, while the concentration of black carbon decreases with increasing temperature (not shown). Such relationships can not be generalized and depend on the local relative contributions of the PM components. In addition, the large scatter indicates that the relationship between PM and meteorology is complex and that using only temperature as a proxy for meteorological conditions does not suffice to explain all observed variation.

Maximum ozone concentrations are reached in summer since ozone is formed by photochemical reactions. For PM_{10}, the annual cycle depends on the exact composition which varies per location. To investigate the annual cycle and in which periods the impact of climate change is largest, we analyzed the 20-yr records of simulated monthly means of daily mean PM_{10} concentrations, which are shown for Vredepeel and Madrid (Fig. 11). PM_{10} concentrations tend to be lowest in summer. Some locations show distinct periods of higher concentrations in spring/autumn (Melpitz, Els Torms), while others show a more gradual increase in the winter half year. For Madrid, high PM_{10} concentrations are a winter phenomenon. The highest concentrations are seen in the RLE_ERA run, which has the lowest wind speeds and the least amount of precipitation in the winter months. Vredepeel however, has rather high PM_{10} concentrations in early spring and late summer. This can be related partly to the relatively high ammonia emission in this area in these periods, and partly to wind speed, in particular for the RLE_MIROC future climate, which has the lowest wind speeds in late summer. Both RLE_MIROC and RLE_ECHAM show that PM_{10} concentrations may increase due to climate change for late summer in Vredepeel. For Madrid, RLE_MIROC and RLE_ECHAM predict concentration changes of up to $2\,\mu g\,m^{-3}$ due to climate change, but with opposite signs: future PM_{10} concentrations will decrease according to RLE_MIROC and increase according to RLE_ECHAM. Most other rural locations that were analyzed show maximum concentrations in early spring and autumn, with a negligible impact of climate change. Figure 11 shows

that differences in annual mean concentrations between the runs and periods can be lower than the differences in monthly mean concentrations, and that the main impact of climate change may be observed in a specific season, depending on the region.

5 Discussion and conclusions

Two long-term climate simulations have been performed with the one-way coupled system RACMO2-LOTOS-EUROS, using meteorological boundary conditions from two different GCMs to study the impact of climate change on air quality. In addition, a 21-yr present-day simulation was performed using boundary conditions from reanalysis meteorology, which served as a reference for the the present-day period air quality modeled by the two climate simulations. The two climate simulations using ECHAM and MIROC forcings differ significantly from the reference using ERA-Interim but also from each other, primarily owing to the differences in circulation patterns (meteorology).

The results of the two long-term simulations were used to compute the difference in air quality between the present-day (1989–2009) and the future climate (2041–2060). The difference in meteorology between future and present-day climate is mainly a considerable increase in temperature, whereas the circulation pattern, rain and wind show only a modest change. The increase in temperature yields an increase in mean daily summer maximum ozone concentrations of up to $12\,\mu g\,m^{-3}$. Above the Northern Atlantic mean PM_{10} concentrations are up to 1–$2\,\mu g\,m^{-3}$ lower in future than in the present day climate. Over the continent changes are around $0.5\,\mu g\,m^{-3}$, with positive changes over the Netherlands, North-West Germany, North-East Spain and the Po valley. Results from the two simulations are in agreement regarding general response (general increase in ozone concentration, weak response of PM_{10}), however, there are considerable differences in absolute values and between regions. For some regions the two models did not even agree on the sign of the change in PM_{10}. However, at most locations changes in PM_{10} are not significant.

The results obtained in this paper cannot be compared with results from literature in a straightforward way, due to the differences in metrics used (e.g. average 8-h maximum, averages over April–September, AOT40), the difference in time windows (most used are 1961–1990, 2071–2100), and differences in climate scenario (A2, A1B). Nevertheless, the results of this study appear to be generally in line with European studies (e.g. Giorgi and Meleux 2007, up to 10 ppbv difference in mean daily summer ozone concentrations, Andersson et al., 2009, up to 7 ppbv difference in mean daily maximum O_3 with future climate representing 2021–2050, Carvalho et al., 2010 are at the high end with up to $50\,\mu g\,m^{-3}$ difference in monthly mean O_3 concentrations) and US studies (see the overview by Jacob and Winner, 2009). For PM, usually annual or seasonal means are reported, sometimes given per component, with both increases and decreases of up to 10 %, or less than $1\,\mu g\,m^{-3}$ (Jacob and Winner, 2009). Thus our results comply with results from literature. However, they also indicate a considerable sensitivity to the choice of the global climate model that serves as a driver for the air quality simulations.

The changes in concentrations of ozone and PM_{10} can be related to changes in temperature, i.e. daily maximum temperature, and to a lesser extent to changes in precipitation and wind speed. Average relationships between concentrations and temperature differ slightly between the different simulations and time windows. This implies that average relationships for the present-day climate cannot be directly extrapolated to the future. Furthermore, changes are not uniform over the year. High ozone concentrations are clearly a summer phenomenon but for PM_{10} the seasonal behavior is less uniform. In the Netherlands, for example, an increase in summertime PM_{10} seems a robust feature, but for other seasons the changes appear smaller. For Madrid, on the other hand, the model simulations indicate that high PM_{10} concentrations are mainly a winter phenomenon. This implies that although one could in principle carry out a bias correction for the portion of the climate simulation that represents the present-day climate, this bias correction would only be valid locally and would only be applicable to the future climate to a limited extent.

The meteorological parameters from both climate simulations (RLE_ECHAM and RLE_MIROC) differ considerably from those of the reanalysis-driven simulation RLE_ERA for the period 1989–2009, depending on the season and region, even though both ECHAM5 and MIROC are among the better-performing global climate models (Van Ulden and Van Oldenborgh, 2006). These differences have a substantial impact on the modeled ozone and PM_{10} concentrations. For the RLE_ECHAM run, differences in modeled concentrations between future and present-day climate are smaller than the differences in present-day climate between RLE_ECHAM and RLE_ERA. In the RLE_MIROC simulation, the differences between future and present-day climate are of the same order of magnitude as the present-day differences between the simulations of RLE_MIROC and RLE_ERA. Yet, differences between either RLE_ECHAM or RLE_MIROC and RLE_ERA have divergent characteristics, illustrating the uncertainties in the global climate models. Results from a single transient simulation should therefore be interpreted in a qualitative rather than a quantitative way, merely as an illustration of one out of many possible climate change realizations. The two simulations analyzed in this paper show differences, but also consistent changes related to climate change. Nevertheless, ideally an ensemble approach should be taken, with ensemble members from different GCMs and different regional climate models.

In this paper only the impact of differences in meteorology has been considered. However, chemistry transport models

also have biases, and an ideal ensemble should include several CTMs as well. LOTOS-EUROS underestimates the daily ozone maximum (Curier et al., 2012). In particular the highest ozone peaks ($180\,\mu g\,m^{-3}$) are underestimated by 10–$20\,\mu g\,m^{-3}$. It also underestimates total PM_{10}, especially in summer (Manders et al., 2009). In Mues et al. (2012) the relation between temperature and PM_{10} concentrations was investigated for LOTOS-EUROS and compared with observed concentrations. The observed increase in PM concentrations with temperature was not represented to the same extent by the model. For winter periods, during which PM is mainly determined by ventilation effects, the behavior is fairly good, but for summertime conditions the model is not performing adequately. LOTOS-EUROS lacks a good description of SOA, which may contribute significantly (typically up to a few $\mu g\,m^{-3}$) in summer through the temperature dependency of biogenic emissions and the dependency on photochemistry (oxidation) and volatility (Donahue et al., 2009 and references therein). Windblown dust will be more important under warmer and dryer conditions, in particular in Southern Europe, but is currently not taken into account. Furthermore, the contribution of forest fire emissions is not modeled. Forest fires can contribute significantly to ozone and PM concentrations during fire episodes and can cause serious and acute local air quality problems. Through long-range transport of emissions, forest fires have an impact on atmospheric conditions at distances of hundreds of kilometers away from the fire, not only on the concentrations but also on the radiation budget and atmospheric stability (e.g. Hodzic et al., 2007; Saarikoski et al., 2007). The emissions of forest fires are expected to increase for a warmer climate in the Mediterranean area (e.g. Moriondo et al., 2006). Therefore we must state that the changes in concentration in response to changes in meteorology as considered in this study are probably an underestimation of the impact of climate change on air quality.

In the present study, anthropogenic emissions have been kept constant at the 2005 level to focus on the impact of meteorology. The interannual variability in concentration is largely due to meteorological variability rather than interannual variability in emissions (Andersson et al., 2007), but the effect of changes in emissions between 2000 and 2050 on the long-term average concentrations may be as large as or even larger than the effect of climate change (Tagaris et al., 2007). Not only the amount of emissions, but also their timing may change due to changes in energy sources and in human activity patterns. The increase of observed elemental carbon concentrations with higher temperatures was not reproduced by LOTOS-EUROS (Mues et al., 2012), which may indicate an effect of meteorology on anthropogenic emissions. Emission scenarios should be taken into account when assessing air quality for a future period, in particular for the strong emission reductions expected for Europe for the coming decades.

Other sources of uncertainty in the interactions between climate change and air quality are the boundary conditions, enhanced stratosphere-troposphere exchange and higher background levels. Andersson et al. (2009) conducted an impact study, and Hogrefe et al. (2011) studied the uncertainties associated with chemical boundary conditions from a global model, showing that the interannual variability was underestimated when time-invariant boundary conditions were used. Also land use changes may be relevant as they affect deposition efficiencies and biogenic emissions, although their effect may be small. And last but not least, two-way interactions between concentrations of species and the radiation budget of the atmosphere should be taken into account (Zhang et al., 2010). Unfortunately, most present-day coupled models are not capable of performing long-term climate studies due to the large computational effort that would be required. A two-way coupling approach with relatively modest computational demands is currently being realized in the RACMO2-LOTOS-EUROS system.

Supplementary material related to this article is available online at: http://www.atmos-chem-phys.net/12/9441/2012/acp-12-9441-2012-supplement.pdf.

Acknowledgements. This project was supported by the Dutch Knowledge for Climate Programme. We thank two anymous reviewers for their constructive comment.

Edited by: P. Jöckel

References

Andersson, C.: Air pollution dependency on climate variability and source region, PhD. Thesis, Stockholm University, 2009.

Andersson, C., Langner, J., Bergstrom, R. Interannual variations and trends in air pollution over Europe due to climate variability during 1958–2001 simulated with a regional CTM coupled to the ERA-40 reanalysis, Tellus 59B, 77–98, 2007.

Bergström, R., Denier van der Gon, H. A. C., Prévôt, A. S. H., Yttri, K. E., and Simpson, D.: Modelling of organic aerosols over Europe (2002–2007) using a volatility basis set (VBS) framework: application of different assumptions regarding the formation of secondary organic aerosol, Atmos. Chem. Phys., 12, 8499–8527, doi:10.5194/acp-12-8499-2012, 2012.

Carvalho, A., Monteiro, A., Solman, S., Miranda, A. I., and Borrego, C.: Climate-driven changes in air quality over Europe by the end of the 21st century, with special reference to Portugal, Environ. Sci. Policy, I3, 445–458, 2010.

Christensen, J. H. and Christensen, O. B.: A summary of the PRUDENCE model projections of changes in European climate by the end of this century, Climate Change, 81, 7–30, 2007.

Curier, R. L., Timmermans, R., Eskes, H., Calabretta-Jongen, S., Segers, A., and Schaap, M.: Improving ozone forecasts over Europe by synergistic use of the LOTOS-EUROS chemical transport model and in-situ measurements, Atmos. Environ., 60, 217–226, 2012.

Dee, D. P., Uppala, S. M., Simmons, A. J., Berrisford, P., Poli, P., Kobayashi, S., Andrae, U., Balmaseda, M. A., Balsamo, G., Bauer, P., Bechtold, P., Beljaars, A. C. M., van de Berg, L., Bidlot, J., Bormann, N., Delsol, C., Dragani, R., Fuentes, M., Geer,

A. J., Haimberger, L., Healy, S. B., Hersbach, H., Hólm, E. V., Isaksen, L., Kållberg, P., Köhler, M., Matricardi, M., McNally, A. P., Monge-Sanz, B. M., Morcrette, J.-J., Park, B.-K., Peubey, C., de Rosnay, P., Tavolato, C., Thépaut, J.-N., and Vitart, F., The ERA-Interim reanalysis: configuration and performance of the data assimilation system, Q. J. Roy. Meteorol. Soc., 137, 553–597, doi:10.1002/qj.828, 2011.

Dentener, F., Stevenson, D., Ellingsen, K., van Noije, T., Schultz, M., Amann, M., Atherton, C., Bell, N., Bergmann, D., Bey, I., Bouwman, L., Butler, T., Cofala, J., Collins, B., Drevet, J., Doherty, R., Eickhout, B., Eskes, H., Fiore, A., Gauss, M., Hauglustaine, D., Horowitz, L., Isaksen, I. S. A., Josse, B., Lawrence, M., Krol, M., Lamarque, J. F., Montanaro, V., Müller, J.F., Peuch, V. H., Pitari, G., Pyle, J., Rast, S., Rodriguez, J., Sanderson, M., Savage, N. H., Shindell, D., Strahan, S., Szopa, S., Sudo, K., Van Dingenen, R., Wild, O., and Zeng, G.: The global atmospheric environment for the next generation, Environ. Sci. Technnol., 40, 3586–3594, doi:10.1021/es0523845, 2006.

Donahue, N. M., Robinson, A. L., and Pandis, S. N.: Atmospheric organic particulate matter: From smoke to secondary aerosol, Atmos. Environ., 43, 94–106, 2009.

EPA: National Ambient Air Quality Standards, available at: http://www.epa.gov/ttn/naaqs/ (last access: 9 October 2012), 2012.

EU Directive 2008/50/EC of the European Parliament and of the Council of 21 May 2008 on ambient air quality and cleaner air for Europe, 2008.

Forkel, R. and Knoche, R.: Nested regional climate-chemistry simulations for central Europe, ComptesRendus – Geoscience 339, 734–746, 2007.

Gelencsér, A., May, B., Simpson,D., Sánchez-Ochoa, A., Kasper-Giebl, A., Puxbaum, H., Caseiro, A., Pio, C., Legrand, M.: Source apportionment of $PM_{2.5}$ organic aerosol over Europe: Primary/secondary, natural/anthropogenic, and fossil/biogenic origin, J. Geophys. Res., 112, D23S04, doi:10.1029/2006JD008094, 2007.

Giorgi, F. and Meleux, F., Modelling the regional effects of climate change on air quality, C. R. Geoscience, 339, 721–733, 2007.

Guenther, A. B., Zimmerman, P. R., Harley, P. C., Monson, R. K., and Fall, R.: Isoprene and monoterpene emission rate variability: model evaluations and sensitivity analyses, J. Geophys. Res., 98, 12609–12617, 1993.

Hodzic, A., Madronich, S., Bohn, B., Massie, S., Menut, L., and Wiedinmyer, C.: Wildfire particulate matter in Europe during summer 2003: meso-scale modeling of smoke emissions, transport and radiative effects, Atmos. Chem. Phys., 7, 4043—4064, doi:10.5194/acp-7-4043-2007, 2007.

Hogrefe, C., Hao, W., Zalewsky, E. E., Ku, J.-Y., Lynn, B., Rosenzweig, C., Schultz, M. G., Rast, S., Newchurch, M. J., Wang, L., Kinney, P. L., and Sistla, G.: An analysis of long-term regional-scale ozone simulations over the Northeastern United States: variability and trends, Atmos. Chem. Phys., 11, 567–582, doi:10.5194/acp-11-567-2011, 2011.

Im, U., Markakis, K., Poupkou, A., Melas, D., Unal, A., Gerasopoulos, E., Daskalakis, N., Kindap, T., and Kanakidou, M.: The impact of temperature changes on summer time ozone and its precursors in the Eastern Mediterranean, Atmos. Chem. Phys., 11, 3847–3864, doi:10.5194/acp-11-3847-2011, 2011.

Im, U., Markakis,K., Koçak, M., Gerasopoulos, E., Daskalakis, N., Mihalopoulos, N., Poupkou, A., Kindap, T., Unal, A., and Kanakidou, M.: Summertime aerosol chemical composition in the Eastern Mediterranean and its sensitivity to temperature, Atmos. Environ., 50, 164–173, doi:10.1016/j.atmosenv.2011.12.044, 2012.

IPCC: Contribution of Working Groups I, II and III to the Fourth Assessment Report of the Intergovernmental Panel on Climate Change Core Writing Team, edited by: Pachauri, R. K. and Reisinger, A., IPCC, Geneva, Switzerland, pp. 104, 2007.

Jacob, D. J. and Winner, D. A.: Effect of climate change on air quality, Atmos. Environ., 43, 51–63, 2009.

Jacob, D., Barring, L., Christensen, O. B., Christensen, J. H., de Castro, M., Deque, M., Giorgi, F., Hagemann, S., Hirschi, M., Jones, R., Kjellstrom, E., Lenderink, G., Rockel, B., Sanchesz, E., Schar, C., Seneviratne, S. I., Somot, S., van Ulden, A., and Van den Hurk, B.: An inter-comparison of regional climate models for Europe: model performance in present-day climate, Climatic Change, 81, 31–52, 2007.

Jimenez-Guerrero, P., Jose Gomez-Navarro, J., Jerez, S., Lorente-Plazas, R., Garcia-Valero, J. A., and Montavez, J. P.: Isolating the effects of climate change in the variation of secondary inorganic aerosols (SIA) in Europe for the 21st century (1991–2100), Atmos. Environ., 45, 1059–1063, 2011.

Jungclaus, J. H., Botzet, M., Haak, H., Keenlyside, N., Luo, J. J., Latif, M., Marotzke, J., Mikolajewicz, U., and Roeckner, E.: Ocean circulation and tropical variability in the AOGCM ECHAM5/MPI-OM, J. Climate, 19, 3952–3972, 2006.

K-1 Model Developers: K-1 Coupled Model (MIROC) Description, K-1 Technical Report 1, edited by: Hasumi, H. and Emori, S., Center for Climate System Research, University of Tokyo, Tokyo, Japan, 34 pp., available at: http://www.ccsr.u-tokyo.ac.jp/kyosei/hasumi/MIROC/tech-repo.pdf, 2004.

Kjellström, E., Boberg, F., Castro, M., Christensen, H. J., Nikulin, G., and Sánchez, E.: Daily and monthly temperature and precipitation statistics as performance indicators for regional climate models, Clim. Res., 44, 135–150, 2010.

Kuenen, J., Denier van der Gon, H., Visschedijk, A., Van der Brugh, H., and Van Gijlswijk, R.: MACC European emisison inventory for the years 2003–2007, TNO report, UT-2011-00588, 2011.

Lenderink, G., Van den Hurk, B., Van Meijgaard, E., Van Ulden, A. P., and Cuijpers, J.: Simulation of present-day climate in RACMO2: first results and model developments, KNMI technical report TR 252, 2003.

Liao, K.-J., Tagaris, E., Manomaiphiboon, K., Wang, C., Woo, J.-H., Amar, P., He, S., and Russell, A. G.: Quantification of the impact of climate uncertainty on regional air quality, Atmos. Chem. Phys., 9, 865–878, doi:10.5194/acp-9-865-2009, 2009.

Manders, A. M. M., Schaap, M., and Hoogerbrugge, R.: Testing the capability of the chemistry transport model LOTOS-EUROS to forecast PM_{10} levels in the Netherlands, Atmos. Environ., 43, 4050–4059, 2009.

Manders, A. M. M., van Ulft, B., van Meijgaard, E., and Schaap, M.: Coupling of the air quality model LOTOS-EUROS to the climate model RACMO, Dutch National Research Programme Knowledge for Climate Technical Report KFC/038E/2011, ISBN 978-94-90070-00-7, 2011.

Metzger, S.: Gas/Aerosol Partitioning: A simplified method for global modeling. PhD Thesis, Utrecht University, 2000.

Mitchell, J. F. N., Johns, T. C., Eagles, M., Ingram, W. J., and Davis, R. A.: Towards the construction of climate change scenarios, Cli-

matic Change, 41, 547–581, 1999.

Monahan, E. C., Spiel, D. E., and Davidson, K. L.: A model of marine aerosol generation via whitecaps and wave disruption, in: Oceanic Whitecaps and their role in air/sea exchange, edited by: Monahan, E. C. and Mac Niocaill, G., D. Reidel, Norwell, Mass., USA, 167–174, 1986.

Mues, A., Manders, A., Schaap, M., Kerschbaumer, A., Stern, R., and Builtjes, P.: Impact of the extreme meteorological conditions during the summer 2003 in Europe on particle matter concentrations – an observation and model study. Atmos. Environ., 55, 377–391, 2012.

Moriondo, M., Good, P., Durão, R., Bindi, M., Giannakopoulos, C., and Corte-Real, J.: Potential impact of climate change on fire risk in the Mediterranean area, Clim. Res., 31, 85–95, doi:10.3354/cr031085, 2006.

Raes, F., Liao, H., Chen, W.-T., and Seinfeld, J. H.: Atmospheric chemistry-climate feedbacks, J. Geophys. Res., 115, D12121, doi:10.1029/2009JD013300, 2010.

Roeckner, E., Bäuml, G., Bonaventura, L., Brokopf, R., Esch, M., Giorgetta, M., Hagemann, S., Kirchner, I., Kornblueh, L., Manzini, E., Rhodin, A., Schlese, U., Schulzweida, U., and Tompkins, A.: The Atmospheric General Circulation Model ECHAM5, Part I: Model Description, MPI Report 349, Max Planck Institute for Meteorology, Hamburg, Germany, 127 pp., 2003.

Saarikoski, S., Sillanpaa, M., Sofiev, M., Timonen, H., Saarnio, K., Teinila, K., Kukkonen, J., and Hillamo, R.: Chemical composition of aerosols during a major biomass burning episode over northern Europe in spring 2006: Experimental and modeling assessments, Atmos. Environ., 41, 3577–3589, 2007.

Schaap, M., Timmermans, R. M. A., Sauter, F. J., Roemer, M., Velders, G. J. M., Boersen, G. A. C., Beck, J. P., and Builtjes, P. J. H.: The LOTOS-EUROS model: description, validation and latest developments, Int. J. Environ. Pollut., 32, 270–290, 2008.

Solazzo, E., Bianconi, R., Vautard, R., Appel, K. W., Moran, M. D., Hogrefe, C., Bessagnet, B., Brandt, J., Christensen, J. H., Chemel, C., Coll, I., Denier van der Gon, H., Ferreira, J., Forkel, R., Francis, X. V., Grell, G., Grossi, P., Hansen, A. B., Jerièeviæ, A., Kraljeviæ, Miranda, A. I., Nopmongcol, U., Pirovano, G., Prank, M., Riccio, A., Sartelet, K. N., Schaap, M., Silver, J. D., Sokhi, R. S., Vira, J., Werhahn, J., Wolke, R., Yarwood, G., Zhang, J., Rao, S. T., and Galmarini, S.: Model evaluation and ensemble modelling of surface-level ozone in Europe and North America in the context of AQMEII, Atmos. Environ., 53, 60–74, doi:10.1016/j.atmosenv.2012.01.003, 2012.

Tagaris, E., Manomaiphiboon, K., Liao, K.-J., Leung, L. R., Woo, J. H., He, S., Amar, P., and Russell, A. G.: The impact of global climate change and emissions on regional ozone and fine particulate matter concentrations over the US, J. Geophys. Res.-Atmos., 112, D14312, doi:10.1029/2006JD008262, 2007.

Tai, A. P. K., Mickely, L. R., and Jacob, D. J.: Correlations between fine particulate matter ($PM_{2.5}$) and meteorological variables in the United States: implications for the sensitivity of $PM_{2.5}$ to climate change, Atmos. Environ., 44, 3976–3984, doi:10.1016/j.atmosenv.2010.06.060, 2010.

Undén, P. et al.: HIRLAM-5 Scientific Documentation, available from SMHI, S-601 76 Norrköping, Sweden, 144 pp., 2002.

Van Loon, M., Vautard, R., Schaap, M., Bergstrom, R., Bessagnet, B., Brandt, J., Builtjes, P. H. J., Christensen, H. J., Cuvelier, C., Graff, A., Jonson, J. E., Krol, M., Langner, J., Roberts, P., Rouil, L., Stern, R., Tarrason, L., Thunis, P., Vignati, E., White, L., and Wind, P.: Evaluation of long-term ozone simulations from seven regional air quality models and their ensemble, Atmos. Environ., 41, 2083–2097, 2007.

van Meijgaard, E., Van Ulft, L. H., Van de Berg, W. J., Bosveld, F. C., Van den Hurk, B. J. J. M., Lenderink, G., and Siebesma, A. P.: The KNMI regional atmospheric climate model RACMO version 2.1, KNMI Technical report, TR-302, 2008.

van Meijgaard, E., Van Ulft, L. H., Lenderink, G., de Roode, S. R., Wipfler, L., Boers, R., and Timmermans, R. M. A.: Refinement and application of a regional atmospheric model for climate scenario calculations of Western Europe, Climate changes Spatial Planning publication: KvR 054/12, ISBN/EAN 978-90-8815-046-3, pp. 44, 2012.

van Ulden, A. P. and van Oldenborgh, G. J.: Large-scale atmospheric circulation biases and changes in global climate model simulations and their importance for climate change in Central Europe, Atmos. Chem. Phys., 6, 863–881, doi:10.5194/acp-6-863-2006, 2006.

Vautard, R., Beekmann, M., Desplat, J., Hodzic, A., and Morel, S.: Air quality in Europe during the summer of 2003 as a prototype of air quality in a warmer climate, C. R. Geoscience, 339, 747–763, 2007a.

Vautard, R., Builtjes, P. H. J., Thunis, P., Cuvelier, P., Bedogni, M., Bessagnet, B., Honore, C., Moussiopoulos, N., Pirovano, G., Schaap, M., Stern, R., Tarrason, L., and Wind, P.: Evaluation and intercomparison of Ozone and PM_{10} simulation by several chemistry transport models over four European Cities within the City Delta project, Atmos. Environ., 41, 173–188, 2007b.

Zhang, Y., Wen, X.-Y., and Jang, C. J.: Simulating chemistry-aerosol-cloud-radiation-climate feedbacks over the continental US using the online-coupled Wather Research Forecasting Model with chemistry (WRF/Chem), Atmos. Environ., 44, 3568–3582, 2010.